Coastal warming under climate change: Global, faster and heterogeneous

R. Varela [a,b,*], M. de Castro [a,b], J.M. Dias [b], M. Gómez-Gesteira [a,b]

[a] *EphysLab - Environmental Physics Laboratory, CIM-UVIGO, Universidade de Vigo, Edificio Campus da Auga, 32004 Ourense, Spain*
[b] *CESAM - Centre for Environmental and Marine Studies, Department of Physics, University of Aveiro, 3810-193 Aveiro, Portugal*

HIGHLIGHTS

- Evaluation of the projected changes in the timing and spatial distribution of the coastal SST
- Warming expected to be global, faster, and more heterogeneous than in previous decades
- All basins show an increase in coastal SST near 1 °C for mid-century relative to 1995–2014.

GRAPHICAL ABSTRACT
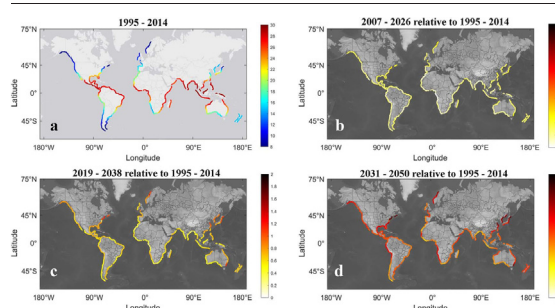
Warming is expected to be global, faster and more heterogeneus for mid-century than for the previous decades

ARTICLE INFO

ABSTRACT

The assessment of expected changes in coastal sea surface temperature (SST) on a global scale is becoming increasingly important due to the growing pressure on coastal ecosystems caused by climate change. To achieve this objective, 17 Global Climate Models from CMIP6 were used, with data from historical and hist-1950 experiments spanning 1982–2050. This analysis highlights significant warming of coastal areas worldwide, with higher and more variable rates of warming than observed in previous decades. All basins are projected to experience an increase in coastal SST near 1 °C by mid-century, with some regions exhibiting nearshore SST anomalies exceeding 2 °C for the period 2031–2050 relative to 1995–2014. Regarding the Eastern Upwelling Boundary Systems, only the Canary upwelling system and the southern part of the Humboldt upwelling system manage to show lower-than-average SST warming rates, maintaining, to a certain extent, their ability to buffer global warming.

1. Introduction

Coastal areas are of great importance for marine ecosystems, as they host most of the biodiversity, productivity, fisheries, industry, and recreation (Pauly and Christensen, 1995; Costanza et al., 1997; Gray, 1997; Worm et al., 2009; IPCC, 2014). However, the future of these areas is uncertain, and has generated significant interest among scientists. First, human activities such as overfishing, contamination, and habitat alteration have already had a significant impact on marine ecosystems (Harvey, 2006; Halpern et al., 2008; Watson et al., 2013). Second, climate change is also affecting coastal ecosystems, resulting in increased sea surface temperatures (SST), more frequent marine heatwaves, and ocean acidification, which can impact productivity, fishing, and fish migration (Hoegh-Guldberg and Bruno, 2010; Cheung et al., 2013; Cheung, 2018; Oliver et al., 2021; Smith et al., 2022).

Over the last few decades, researchers have investigated changes in SST and their impacts. It has been observed that global SST warming is occurring, but at different rates at the local level, emphasizing the importance of conducting regional-scale studies (Lima and Wethey, 2012; García-Reyes et al., 2015; Varela et al., 2018). While many studies have investigated the effects of warming in large marine systems such as the Indian, Pacific, and Atlantic Oceans (Hoegh-Guldberg et al., 2014), fewer studies

---

* Corresponding author at: EphysLab - Environmental Physics Laboratory, CIM-UVIGO, Universidade de Vigo, Edificio Campus da Auga, 32004 Ourense, Spain.
  E-mail address: ruvarela@uvigo.es (R. Varela).

have specifically focused on coastal areas. However, it is important to note that coastal ecosystems, including coral reefs, rocky shores, and estuaries, as well as industries such as coastal aquaculture or rafts, are already experiencing the effects of global warming and facing increasing pressures (Hoegh-Guldberg, 2018; Cooley et al., 2022; Ahmed et al., 2019; Galappaththi et al., 2020; Des et al., 2022).

Therefore, it is critical to evaluate future changes in SST close to the coast, as they can negatively affect different ecosystems. For this purpose, high-resolution databases are needed that accurately reproduce the particular characteristics of areas near the coast. While General Circulation Models (GCMs) of the Coupled Model Intercomparison Project Phase 5 (CMIP5) (Taylor et al., 2012) have been used to assess projected SST data, their coarse spatial resolution (not <1°) did not allow for the accurate representation of local areas such as Eastern Boundary Upwelling Systems (EBUS) (Wang et al., 2014; Ma et al., 2019). The new phase 6 of the CMIP project has been launched to improve the ability to reproduce physical processes, including high-resolution GCMs with spatial resolutions up to 0.1° (Haarsma et al., 2016). These GCMs have shown an improvement in their ability to reproduce SST, with lower mean coastal biases that are directly related to the upgraded GCM resolution (Li et al., 2020; Richter and Tokinaga, 2020; Balaguru et al., 2021; Farneti et al., 2022; Varela et al., 2022a, 2022b; Wang et al., 2022).

The aim of this study is to analyze the expected changes in the timing and spatial distribution of the coastal SST for the Atlantic, Pacific and Indian basins from 1982 to 2050. To achieve this goal, 17 CMIP6 GCMs from the historical and hist-1950 experiments with sufficient resolution to capture the specific characteristics of the coastal systems have been used. Additionally, an SST bias correction has been conducted to minimize any biases related to the CMIP6 models. The National Oceanic and Atmospheric Administration Optimum Interpolation Sea Surface Temperature (NOAA OISST1/4) high-resolution database from 1982 to 2014 has also been utilized in this study, as it has been extensively employed in evaluating SST over the past few decades (Lima and Wethey, 2012; Benazzouz et al., 2014; Varela et al., 2018; Seabra et al., 2019).

2. Methods

2.1. Data

2.1.1. Reference data

Daily SST data was retrieved from the NOAA OISST1/4 database from 1982 to 2014, with a resolution of 0.25° (https://www.ncdc.noaa.gov/oisst). The data was then averaged at a monthly scale. OISST1/4 data have already been used by several authors to reproduce SST patterns near the coast (Lima and Wethey, 2012; Varela et al., 2018).

2.1.2. Modeled data

Monthly SST data were retrieved from the Coupled Model Intercomparison Project Phase 6 (CMIP6) (https://esgf-node.llnl.gov/projects/cmip6/). In particular, results from 17 GCMs, including the High-Resolution Model Intercomparison Project (HighResMIP), were analyzed for the period 1982–2050, with resolutions up to 0.1° (Eyring et al., 2016; Haarsma et al., 2016). Due to the different horizontal resolutions from the CMIP6 GCMs, a bilinear interpolation was carried out to standardize the SST data onto a common 0.25° × 0.25° grid, which matches the OISST1/4 data. A comprehensive outline of the CMIP6 GCMs is provided in Table 1.

2.2. Experiments

Depending on the experiment_id, the availability of CMIP6 GCMs can differ. These experiments vary in aspects such as spatial and temporal resolution, as well as future scenarios considered. For this study, the historical and hist-1950 experiments were utilized.

The historical experiment includes model results from 1850 to 2014, with atmospheric and oceanic resolutions ranging from 0.25° to 1°. Future model data for this experiment corresponds to the SSP5–8.5 experiment,

Table 1

List of the Global Climate Models (GCMs) considered in the present study. These GCMs come from both the historical and hist-1950 experiments of the CMIP6 project.

Model number	Name	Experiment ID	Oceanic resolution (°)	Atmospheric resolution (°)
1	AWI-CM-1-1-MR	Historical	0.25	1
2	CNRM-CM6-1-HR	Historical	0.25	1
3	GFDL-CM4	Historical	0.25	1
4	GFDL-ESM4	Historical	0.5	1
5	HadGEM3-GC31-MM	Historical	0.25	1
6	MPI-ESM1-2-HR	Historical	0.5	1
7	CESM1-CAM5-SE-HR	Hist-1950	0.1	0.25
8	CMCC-CM2-HR4	Hist-1950	0.25	1
9	CMCC-CM2-VHR4	Hist-1950	0.25	0.25
10	CNRM-CM6-1-HR	Hist-1950	0.25	1
11	EC-Earth3P	Hist-1950	1	0.8
12	EC-Earth3P-HR	Hist-1950	0.25	0.5
13	FGOALS-f3-H	Hist-1950	0.1	0.25
14	HadGEM3-GC31-HH	Hist-1950	0.1	0.5
15	HadGEM3-GC31-HM	Hist-1950	0.25	0.5
16	MPI-ESM1-2-HR	Hist-1950	0.5	1
17	MPI-ESM1-2-XR	Hist-1950	0.5	0.5

which represents emissions high enough to produce an 8.5 W m^{-2} level of forcing in 2100. Additional information on this experiment can be found at https://view.es-doc.org/?renderMethod=name&project=cmip6&type=cim.2.designing.NumericalExperiment&client=esdoc-url-rewrite&name=historical

On the other hand, the hist-1950 experiment is part of the High-Resolution Model Intercomparison Project (HighResMIP), which includes models at both high and standard horizontal resolutions (up to 0.1°) from 1950 to 2014. The future model data for this experiment corresponds to the highres-future experiment, covering a temporal period from 2015 to 2050. Additional information on this experiment can be found at https://view.es-doc.org/?renderMethod=name&project=cmip6&type=cim.2.designing.NumericalExperiment&client=esdoc-url-rewrite&name=hist-1950

Studies published recently have examined the ability of CMIP6 GCMs to accurately reproduce SST patterns. Many of these studies have reported improvements in SST representation due to the increased resolution of GCMs (Bock et al., 2020; Li et al., 2020; Richter and Tokinaga, 2020; Balaguru et al., 2021; Farneti et al., 2022; Varela et al., 2022a, 2022b; Wang et al., 2022). However, SST bias reduction is heterogeneous and zone-dependent (Sylla et al., 2022; Varela et al., 2022b). Therefore, this study employs both experiments, although hist-1950 has higher resolution. Verifying that both experiments produce "similar" results, figures similar to Figs. 3, 5, and 6, but related to the historical experiment, are included as Supplementary Material.

2.3. SST bias correction

As previously noted, the existence of biases in the CMIP6 GCMs is well-established (Park and Latif, 2020; Fox-Kemper et al., 2021). Fox-Kemper et al. (2021) obtained significant SST biases from 1995 to 2014 in the multi-model mean of low and high resolution CMIP6 models. Although their study is not focus on coastal regions, it shows significant SST biases in areas such as upwelling regions.

Fig. S1 in the Supplementary Material depicts the coastal SST biases for the multi-model mean of the historical and hist-1950 experiments, revealing the highest SST biases in upwelling regions such as Benguela, Humboldt (especially in Peru), and California, with values reaching up to 3 °C. Additionally, areas such as the Northeastern Pacific Ocean and West Pacific Ocean display SST biases of around 1 °C. These results underscore the challenges faced by CMIP6 models in accurately reproducing coastal SST patterns in these regions (Varela et al., 2022b).

In order to minimize biases, a bias correction procedure was implemented using a Quantile-Quantile calibration method (also known as

Distribution Mapping) based on the quantil mapping (QM) approach. Essentially, this involves adjusting the cumulative distribution function of the modeled data (obtained from CMIP6 GCMs) to match that of the observed data (OISST1/4). For more detailed information on this method, refer to the study of Amengual et al. (2012) and Costoya et al. (2020).

Finally, a multi-model mean was computed for each experiment using the CMIP6 GCMs.

2.4. Selection of the coastal pixels

In this study, coastal locations were identified as the grid points closest to the coast with a SST value from CMIP6 and OISST1/4 datasets. To ensure that the selected pixels accurately represent coastal patterns, only those available from CMIP6 GCMs with a nominal resolution lower than 1° were included. Furthermore, only pixels with >75 % of monthly SST values available during the study period were considered. Fig. 1 displays the coastal pixels selected for each basin. Over 3000 nearshore locations were assessed in this study.

3. Results

>3000 coastal locations were analyzed corresponding to the eastern and western Atlantic, Pacific and Indian basins (East Atlantic (EA), West Atlantic (WA), East Pacific (EP), West Pacific (WP), West Pacific Islands (WPI), East Indian (EI) and West Indian (WI), from now on). Fig. 2 displays the SST averaged for all points of each basin from 1982 to 2050. All basins experienced a clear warming trend by mid-century, although the warming was already apparent during the common reference period of 1982–2014, albeit at a slower rate. For the EA (Fig. 2a), warming SST trends of around 0.21 ± 0.04 °C dec^{-1} have been observed until 2014 which are similar to that obtained by Lima and Wethey (2012) (0.27 °C dec^{-1}) from 1982 to 2010. However, from 2015 to 2050 the CMIP6 multi-model mean indicates a more rapid warming trend of 0.36 ± 0.08 °C dec^{-1} from 2015 to 2050. This rate is nearly twice as fast as the observed rates during the reference

period and would result in a temperature increase of over 1 °C by 2050 compared to 2015. Regarding WA (Fig. 2b), the warming during the reference period has been comparatively mild compared to EA, with warming rates of approximately 0.15 ± 0.04 °C dec^{-1}. The lower values may be due to the cooler trends observed in the Florida area, which are connected to alterations in the Gulf Stream's route (Lima and Wethey, 2012; Cheung et al., 2013). However, as with EA, from 2015 to mid-century, the SST rates increase more rapidly (0.31 ± 0.06 °C dec^{-1}), leading to an SST rise of over 1 °C for 2050 relative to 2015. Hoegh-Guldberg et al. (2014) reported a SST increase of 0.41 °C in the Atlantic Ocean from 1950 to 2009, which is comparable to the increase observed in this study from 1982 to 2014 in the nearshore regions. Moreover, Alexander et al. (2018) and Kessler et al. (2022) reported rising warming trends in the Atlantic's large marine ecosystems during both historical and projected periods. EP is the only basin that does not exhibit warming for the OISST1/4 common period (Fig. 2c). This result could be attributed to two factors. Firstly, the impact of El Niño Southern Oscillation (ENSO) which had two strong occurrences in 1982–1983 and 1997–1998 (Huang et al., 2016). Secondly, the effects of the Humboldt and California upwelling systems, which might locally moderate the impact of global warming, particularly through colder tendencies in the Humboldt system (Demarcq, 2009; Gutiérrez et al., 2011; Varela et al., 2018; Seabra et al., 2019). However, there is a discernible warming trend from 2015 to mid-century, with rates averaging around 0.34 ± 0.07 °C dec^{-1}, resulting in SST values that are up to 1.4 °C higher for the mid-century compared to the common period. These values agree with previous studies focused on the Southeastern (Chamorro et al., 2021) and the Northeastern Pacific Ocean where increasing SST trends throughout the 21st century (Overland and Wang, 2007; Alexander et al., 2018) have been associated with the increased frequency of marine heatwaves in the area (Scannell et al., 2016; Oliver et al., 2019). Similar results have been observed for the WP and WPI regions where warming trends are observed in the reference period (around 0.2 ± 0.05 °C dec^{-1}), which further increase to exceeding 0.3 ± 0.08 °C dec^{-1} from 2015 to 2050 (Fig. 2d, e). These findings are consistent with those reported in Lima and Wethey (2012)
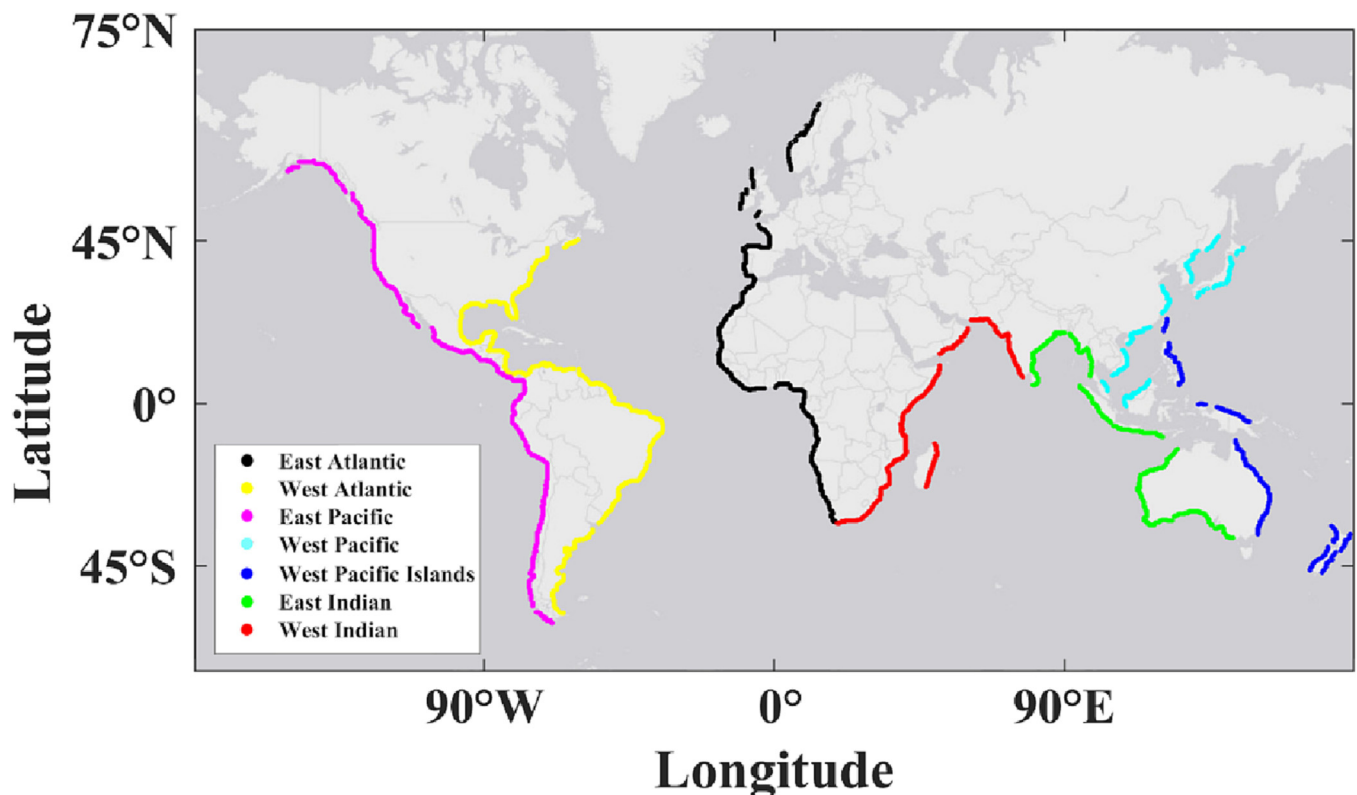

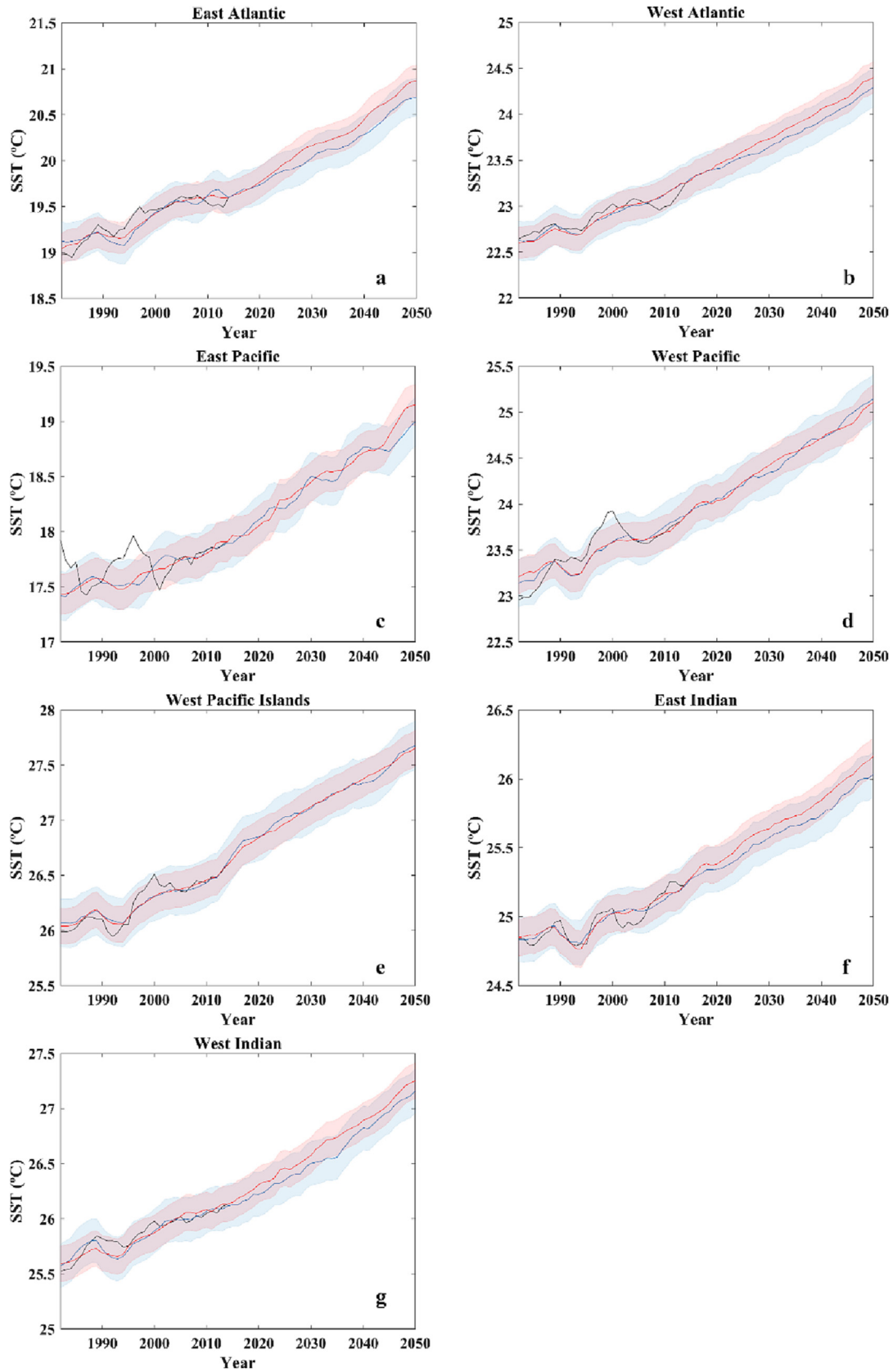**Fig. 1.** Coastal points selected for each basin.

Fig. 2. SST averaged for all points of each basin from 1982 to 2050. Each subfigure displays the multi-model mean of the historical CMIP6 experiment (blue line), multi-model mean of the hist-1950 CMIP6 experiment (red line), and OISST1/4 data (black line from 1982 to 2014). Shadow areas (blue and red) represent the standard deviation of the multi-model mean (historical and hist-1950 experiment, respectively).

and Hoegh-Guldberg et al. (2014), which also showed similar trends for both reference and projected periods. Consistent with earlier research, the Indian Ocean displays the lowest warming compared to other basins (Alory et al., 2007; Lima and Wethey, 2012). On the one hand, the EI basin presents a warming trend of approximately $0.13 \pm 0.04\,°C\,dec^{-1}$ for the reference period (Fig. 2f) while WI basin slightly exceeds it reaching $0.16 \pm 0.05\,°C\,dec^{-1}$ (Fig. 2g). These small discrepancies between both basins have previously been noted by Lima and Wethey (2012) and Hoegh-Guldberg et al. (2014). On the other hand, warming trends from 2015 to mid-century double those from the reference period both for the EI and WI basins ($0.24 \pm 0.07\,°C\,dec^{-1}$ and $0.31 \pm 0.08\,°C\,dec^{-1}$, respectively). Roxy et al. (2020) studied the warming of the Indian Ocean finding an SST increase between 1.2 and 1.6 °C for the period 2040–2069 relative to 1976–2005, which aligns with the results of this study.

Warming trends have been observed in all basins up until mid-century, with varying rates. Furthermore, previous studies (Lima and Wethey, 2012; Varela et al., 2018) have emphasized the need for regional-scale research due to the observed heterogeneity in SST trends. Consequently, Fig. 3 depicts the point-by-point multi-model mean of the SST trend for each basin between 1982 and 2050, utilizing the hist-1950 CMIP6 experiment. The majority of coastal locations worldwide exhibit a warming trend with rates ranging from 0.15 to 0.25 °C dec^{-1}. The Canary upwelling system and the southern section of the Humboldt upwelling system, located along the Chilean coast, exhibit the lowest rates. This observation can have two possible implications. Firstly, it may suggest that these regions will continue to act as a protective barrier against the impacts of global warming, as observed in recent decades (Lima and Wethey, 2012; Santos et al., 2012; Varela et al., 2018). Alternatively, these upwelling areas may lose their capacity to maintain cooling trends near the coast (Varela et al., 2018; Seabra et al., 2019). The Benguela and California upwelling systems exhibit comparable findings, with warming trends not surpassing 0.3 °C dec^{-1}. However, it is essential to acknowledge the limitations of the CMIP6 GCMs in reproducing coastal SST in the EBUS, as noted by Varela et al., 2022b. The same authors also observed that, except for the Canary upwelling system, most CMIP6 GCMs tend to overestimate SST near the shore across all EBUS (Varela et al., 2022a, 2022b). The EI basin also displays the lowest rates, as it has experienced less warming than the WI basin in recent decades (Roxy et al., 2014). The highest SST trends are observable in three locations: Northeast and Northwest Atlantic basin and Northwest Pacific basin, where SST trends range between 0.4 and 0.5 °C dec^{-1}. Kessler et al. (2022) observed similar SST trend patterns in Atlantic basin large marine ecosystems between 1957 and 2020. The Norwegian Sea and North Sea in the East Atlantic basin, as well as the Northeast US Shelf in the West Atlantic basin, experienced the highest total mean SST changes. Meanwhile, Alexander et al. (2018) studied future projected SST

in the North Atlantic Ocean during 1976–2099, using a CMIP5 ensemble mean. They found that the highest warming rates (0.4–0.45 °C dec^{-1}) occurred in the Norwegian Sea (East Atlantic basin), as well as in the Northeast US Shelf and Scotian Shelf (West Atlantic basin). Fox-Kemper et al. (2021) also examined the worldwide SST rate of change from 2005 to 2050 and identified the same regions as previous studies, with the highest SST rates (above 0.6 °C dec^{-1}). East Japan and the Sea of Japan have been historical hotspots for warming, and this trend is predicted to continue towards the mid-century, as noted by Hobday and Pecl (2014) and Dunstan et al. (2018). Ruela et al. (2020) conducted a recent study on SST evolution under climate change from 1970 to 2100, which found that the areas with the highest SST trends (up to 0.5 °C dec^{-1}) are consistent with those identified in the present work. Similar patterns can also be observed in the historical experiment of the CMIP6 project, as depicted in Fig. S2 of the Supplementary Material.

Limiting global warming to 1.5 °C is currently one of the most important objectives, as the unexpected impacts on natural and human systems can be significant, as noted by Hoegh-Guldberg (2018). However, it is expected that the temperature changes in the ocean will be more moderate than those in the atmosphere, as stated by IPCC (2018, 2021). Thus, we have focused in SST changes between 0.5 °C and/or 1 °C. Following the approach of IPCC (2021) and Lee et al. (2021), the modern period (1995–2014) has been chosen as the reference period to calculate SST anomalies (ΔSST) for different periods until 2031–2050. This approach allows us to determine the period in which each basin will experience an increase of 0.5 °C and/ or 1 °C, as illustrated in Fig. 4. Generally, CMIP6 GCMs from the hist-1950 experiment show faster and larger warming than those from the historical experiment. In the case of the EA (Fig. 4a), the ΔSST reaches 0.5 °C for the period 2017–2036 in the hist-1950 experiment, and for 2020–2039 in the historical experiment. However, in this basin, the maximum ΔSST does not reach 1 °C by mid-century. Warming is faster in the WA, with a ΔSST of 0.5 °C being reached for 2015–2034 in the historical experiment, and for 2013–2032 in the hist-1950 experiment. The ΔSST of 1 °C will be reached for 2030–2049 (Fig. 4b). The difference between both basins could be attributed to the presence of the Benguela and Canary upwelling systems in the East Atlantic Ocean, as well as the swift warming occurring in the Northwest Atlantic. The Pacific Ocean, on the other hand, exhibits the most significant and rapid ΔSST. Regarding the EP basin (Fig. 4c), both experiments indicate a 0.5 °C increase by 2015–2034 and a 1 °C increase by 2030–2049. Similar to the Atlantic Ocean, warming is even faster in the West basin. Both, WP and WPI experience a 0.5 °C increase for the periods 2013–2032 and a 1 °C increase for the periods 2027–2046 and 2030–2049, respectively (Fig. 4d, e). Differences can again be attributed to the modulating effects of the Humboldt and California upwelling systems in the East Pacific basin. The coastal basins
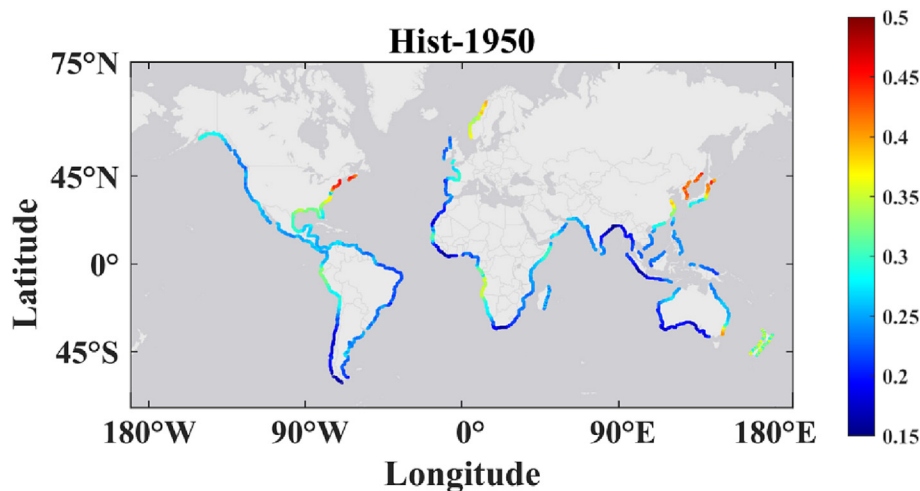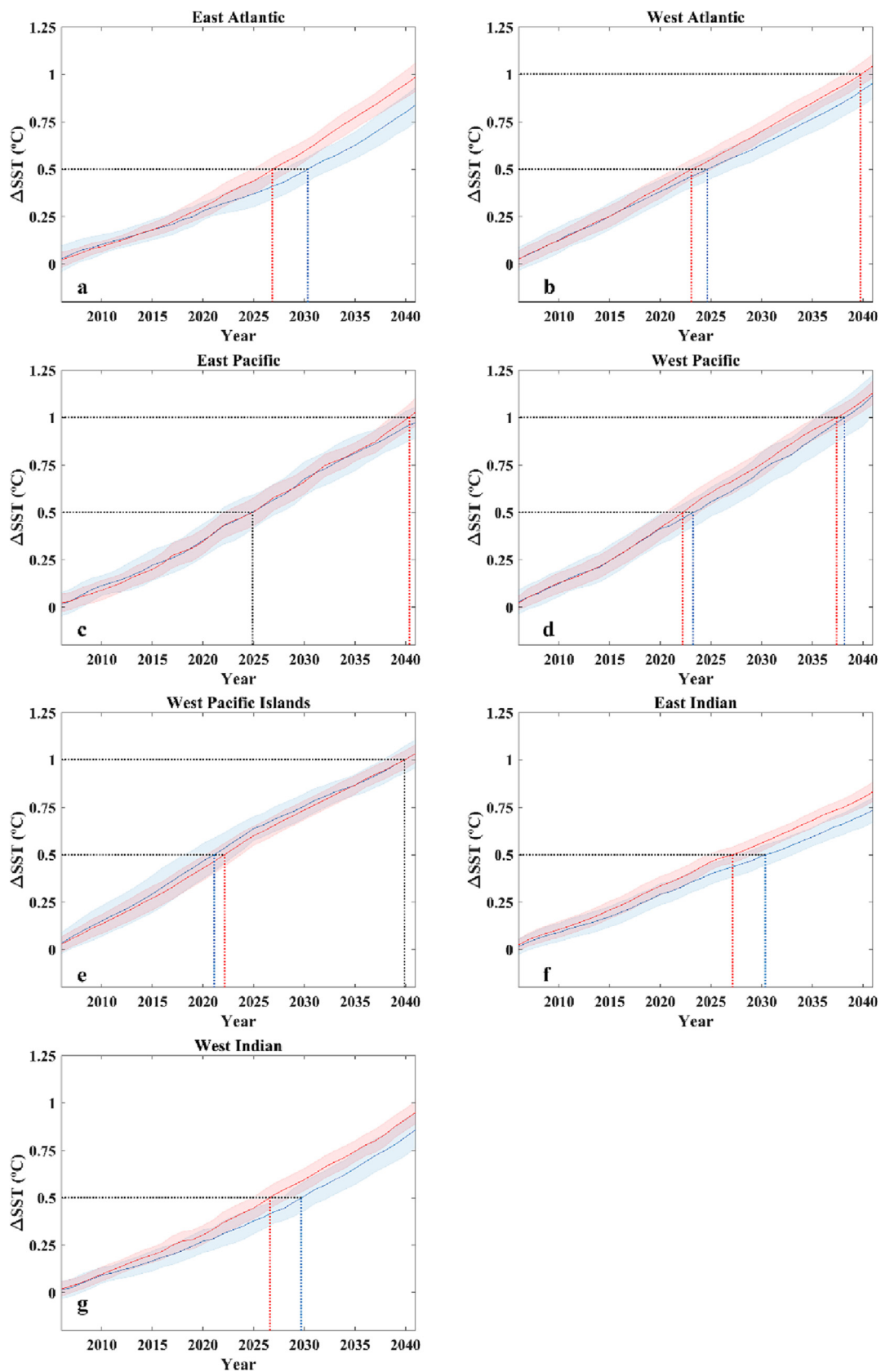

Fig. 3. Multi-model mean of the SST trend (°C dec^{-1}) point-by-point for each basin from 1982 to 2050 for the hist-1950 CMIP6 experiment.

Fig. 4. SST increment (ΔSST) for different periods until 2031–2050 relative to the modern period (1995–2014). The x-axis represents the central year of a 10-year running window. Each subfigure displays the ΔSST multi-model mean of the historical CMIP6 experiment (blue line), and the ΔSST multi-model mean of the hist-1950 CMIP6 experiment (red line). Shadow areas (blue and red) represent the standard deviation of the ΔSST multi-model mean (historical and hist-1950 experiment, respectively). Black dotted line marks the 0.5 °C and 1 °C ΔSST. The blue (red) dotted line indicates the central year of the period in which 0.5 °C and 1 °C of ΔSST will be reached for the historical (hist-1950) experiments. When both experiments reach a ΔSST of 0.5 °C and 1 °C in the same period, the dotted line is black.

Table 2
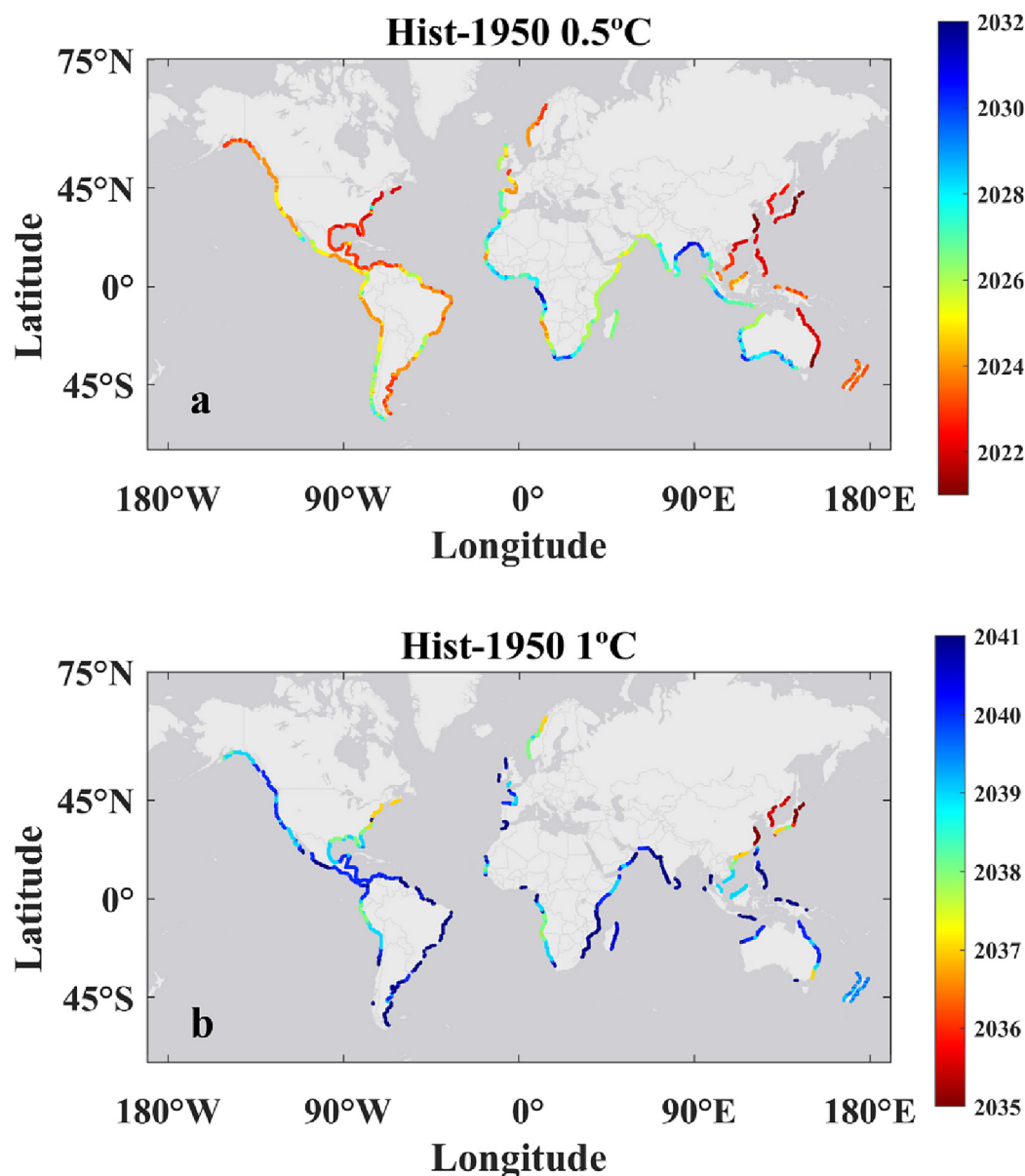Central year of a 10-year running window in which the ΔSST relative to the modern period (1995–2014) is of 0.5 °C or/and 1 °C.

	Historical		Hist-1950	
	0.5 °C	1 °C	0.5 °C	1 °C
East Atlantic	2030	–	2027	–
West Atlantic	2025	–	2023	2040
East Pacific	2025	–	2025	2040
West Pacific	2024	2037	2023	2037
West Pacific Islands	2021	2040	2022	2040
East Indian	2031	–	2028	–
West Indian	2030	–	2027	–

situated in the Indian Ocean, EI and WI, are less affected, with neither exceeding 1 °C by mid-century. EI will attain an ΔSST of 0.5 °C for the historical experiment in the period 2021–2040 and for hist-1950 experiment in the period 2018–2037, as shown in Fig. 4f. The period for WI to reach 0.5 °C ΔSST is 2020–2039 for the historical experiment and 2017–2036 for the hist-1950 experiment, as shown in Fig. 4g. Table 2 provides a

summary of the ΔSST values for various time periods until 2031–2050. The results indicate that an average increase of nearly 1 °C is expected for all coastlines around the world by mid-century. Previous authors studied the expected changes in SST in larger oceanic areas. Brown et al. (2015) evaluated the projected SST in the equatorial Pacific. They found SST anomalies around 2–3 °C for the period 2050–2100 relative to 1950–2000. The study conducted by Ruela et al. (2020) analyzed the differences between the historical SST annual mean (1975–2005) and the near-term future (2020–2050) under the RCP 8.5 climatic scenario. They categorized their findings into eight clusters: Polar cluster (PRN-PRS), Sub-Tropical cluster (STRN-STRS), Tropical cluster (TRN-TRS), and Equatorial cluster (ERN-ERS). The authors observed changes in SST ranging from 0.71 to 1.18 °C, which is consistent with the results obtained in this study.

Fig. 4 previously showed that the expected ΔSST for mid-century is roughly 1 °C across almost all basins, but there are local scale variations in the warming pattern as demonstrated in Fig. 3. To examine the regional behavior of SST patterns, Fig. 5 illustrates the central year of a 10-year running window during which each pixel achieves an ΔSST of 0.5 °C (Fig. 5a)

Fig. 5. Central year of a 10-year running window in which each pixel reaches an ΔSST of a) 0.5 °C and b) 1 °C relative to the modern period (1995–2014) for the hist-1950 CMIP6 experiment.

and 1 °C (Fig. 5b) relative to the modern period (1995–2014). The figures clearly demonstrate the variability in local SST warming rates, even among pixels within the same basin. In the EA region, the fastest SST rates are obtained for the northern section of the Benguela upwelling system and the Norwegian Sea reaching ΔSST over 0.5 °C before 2025. Similar, these zones will be the fastest to exceed an ΔSST of 1 °C (around 2037–2038), while other areas as the Canary upwelling system will not reach that ΔSST. Regarding the WA, the northern section (Scotian Shelf) stands out, with a projected ΔSST exceeding 0.5 °C (1 °C) around 2022 (2037). As for the EP, there are two areas with faster rates of warming than the rest. The first is the northernmost section of the Humboldt upwelling system (Peruvian coast), and the second is the coasts of Canada and Alaska, both expected to exceed a ΔSST of 0.5 °C around 2024–2025 and 1 °C around 2038–2039. The WP and WPI exhibit some of the highest rates of SST warming worldwide. Overall, there is a certain level of homogeneity along all coastlines, with East Japan standing out as the region projected to exceed a ΔSST of 0.5 °C by 2022 and 1 °C by 2035. Conversely, the Indian Ocean displays some of the lowest SST warming rates. In fact, most of the EI does not reach a ΔSST of 1 °C, similar to the Agulhas upwelling system in the WI. Supplementary Fig. S3 corresponds to the historical experiment, which shows similar patterns to the hist-1950 experiment but with more moderate rates of SST warming. In fact, a higher number of coastal pixels in the historical experiment are expected to not reach a ΔSST of 1 °C compared to the hist-1950 experiment.

Fig. 6a shows the distribution of SST for the modern period (1995–2014) using the hist-1950 experiment. The highest SST values are observed in the tropics and lower ones in the northern and southern latitudes. In addition, Fig. 6 (b-d) displays the ΔSST between three different periods (2007–2026, 2019–2038 and 2031–2050), allowing for an assessment of the temporal and spatial distribution of expected SST warming. As expected, warming intensifies over time across all regions (Fig. 6b-d), albeit with variations at the local level. The ΔSST for the period 2007–2026 relative to the modern period is displayed in Fig. 6b. The great majority of nearshore locations show ΔSST values between 0 and 0.5 °C, with no notable differences at the regional scale. However, differences in patterns begin to emerge for the 2019–2038 period (Fig. 6c). Overall, ΔSST ranges

from 0.5 to 0.8 °C, although some areas stand out for exceeding a SST increase of 1 °C. Similar patterns can be observed for the latest period (Fig. 6d). Here, most of the coastal areas show ΔSST around 0.8–1.2 °C. In this case, it should be highlighted the lowest ΔSST observed in the EI, Canary upwelling system and the area of Chile in the Humboldt upwelling system. The differences between the EI and WI may be linked to an ocean-atmosphere feedback mechanism, which causes the expansion of the Indian Ocean warm pool, resulting in the advection of warm waters in the coastal areas of WI (Rao et al., 2012). Regarding the Canary upwelling system, Varela et al. (2022a) reported lower SST warming rates by the end of the century associated with the influence of upwelling in the area. In the case of the Humboldt upwelling system, the southern part (Chile) exhibits lower ΔSST than the northern part (Peru), which displays higher rates. The Norwegian Sea (Northeast Atlantic basin), Scotian Shelf (Northwest Atlantic basin), and the northern and southern areas of the WP display the highest ΔSST values, reaching up to 2 °C. In relation to the Norwegian Sea, previous studies by Stenevik and Sundby, (2007) reported SST increases ranging from 1 to 2 °C for different periods between 2050 and 2075. The Scotian Shelf area is currently known as one of the most important hotspots, and it is expected to experience rapid warming in the future. In fact, Seidov et al. (2021) studied the recent warming in the Gulf of Maine and found that has been a warming acceleration in the recent 10 years attributed to a strengthened northward incursion of warm water in the region. They also observed unprecedented warming in the Scotian Shelf, which may be linked to a change in the pattern of the Gulf Stream extension. The ΔSST value obtained in the this study for the area (around 2 °C) is consistent with previous studies that examined large marine areas (Khan et al., 2013; Ruela et al., 2020; Fox-Kemper et al., 2021). Lastly, there are three regions in the WP that should be noted: East Japan, the Sea of Japan, and Southeast Australia. The projected SST in the Tasman Sea was evaluated by Oliver et al. (2014), who found an SST increase of approximately 2 °C by 2060. These findings were consistent with those of Hobday and Lough (2011), Ruela et al. (2020), and Cooley et al. (2022) for both regions. Similar patterns can also be observed in the historical experiment of the CMIP6 project, as shown in Fig. S4 of the Supplementary Material.
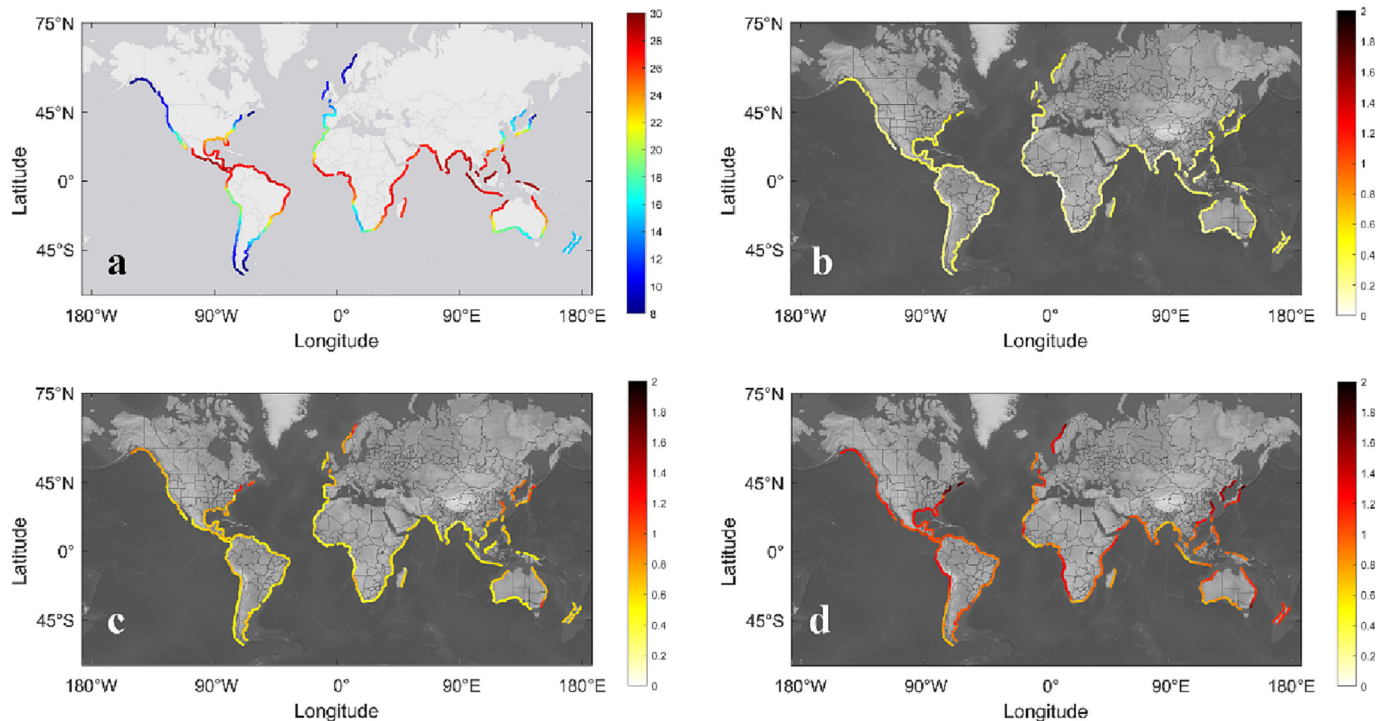

Fig. 6. a) Distribution of SST for the modern period (1995–2014) using the hist-1950 experiment. b-d) ΔSST between three different periods (2007–2026, 2019–2038 and 2031–2050) relative to the modern period using the hist-1950 CMIP6 experiment.

4. Discussion

4.1. Global, faster and non-homogeneous warming

In the AR5 Climate Change 2014: Impacts, Adaptation, and Vulnerability, Hoegh-Guldberg et al. (2014), established that the total SST change in the Atlantic, Pacific, and Indian Oceans was around 0.3–0.6 °C from 1950 to 2009. Here, we have shown that coastal SST is expected to increase globally, faster, and more heterogeneously in the near future than in the past decades.

Firstly, all coastal locations show warming SST trends, which is not necessarily obvious as it was not observed in the last few decades. Studies by Lima and Wethey, (2012) and Varela et al. (2018) found that SST warming trends were observed at around 71–87 % of nearshore locations and SST cooling trends at around 7–13 %. According to the findings of this study, it is projected that by mid-century all basins will undergo an increase in SST.

Secondly, the SST increase is becoming faster. Hansen et al. (2010) concluded that warming trends range between 0.15 and 0.2 °C dec^{-1} at global scales from the 1970s to 2010. Lima and Wethey (2012) estimated an increase of 0.18 °C dec^{-1} from 1982 to 2010 in coastal locations. IPCC (2014) set the SST total change around 0.3–0.6 °C for the Atlantic, Pacific, and Indian Oceans from 1950 to 2009. This study shows that before the 2030s, all basins will experience an SST increase of around 0.5 °C, and by mid-century, the total SST change will exceed 1 °C relative to 1995–2014. Recent studies (Cheng et al., 2019, 2022) also warn of a rapid increase in ocean temperature that will impact nearshore regions.

Thirdly, the SST warming will be non-homogeneous. The areas most affected by projected SST warming are the Norwegian Sea, Scotian Shelf, East Japan and the Sea of Japan, and Southeast Australia, with a total SST change of around 2 °C by mid-century relative to 1995–2014. Previous studies by Belkin (2009), Lima and Wethey (2012), and Kessler et al. (2022) found important regional differences in LMEs warming trends for different historical periods, with the Norwegian Sea, Sea of Japan, and the Labrador and Scotian Shelfs showing the highest warming trends. Focusing on the SST projections, Alexander et al. (2018) studied the future SST in the Northern Oceans from 1976 to 2099. Highest SST trends were also observed in the Norwegian Sea and Scotian Shelf. Conversely, certain regions exhibit lower warming trends in SST with a projected total change of <0.8 °C by mid-century. As reported by Belkin (2009) and Lima and Wethey (2012), the Eastern Indian Ocean experienced a slower rate of change at the continental scale compared to other basins, with an increase of 0.11 °C per decade from 1982 to 2010. The findings of the present study validate a comparable trend in the coming years.

4.2. Causes and consequences of the different SST warming rates

In addition to the heterogeneous warming observed along coastlines worldwide, there is a certain consistency in the distribution of different SST rates for various periods, although the causes of these SST patterns vary locally. For instance, the Norwegian Sea has experienced the fastest SST warming rates due to longer ice-free periods, leading to prolonged absorption of solar radiation and subsequent SST increase (Carvalho and Wang, 2020). This feedback is expected to become more pronounced in the near future. Meanwhile, SST trends in the northwest Atlantic Ocean (Scotian Shelf) are linked to the interaction between the Gulf Stream and the Labrador Current, causing anomalous warm eddies along the Scotian Shelf (Brickman et al., 2018). The causes for the important SST trends in the areas of East China and Japan envelop diverse mechanisms among which stands out the changes in the Kuroshio current which has been accelerated (Sasaki and Umeda, 2021). Moreover, it has been recently observed a weakening in the upwelling at the upstream Kuroshio current, inducing extensive sea surface warming in the area (Wei et al., 2023) On the other hand, the Indian Ocean exhibits lower warming rates, although there are notable differences between the lower SST warming of the eastern basin

and the western basin. This behavior is attributed to the response of the Indian Ocean Dipole to greenhouse warming, creating a positive dipole event that causes faster SST warming in the western basin than the eastern basin (Cai et al., 2013).

4.2.1. Upwelling systems

The response of EBUS to global climate change, including moderate rates of warming or cooling trends, is widely recognized (Belkin, 2009; Lima and Wethey, 2012; Varela et al., 2018; Seabra et al., 2019). For instance, Belkin (2009) observed cooling sea surface temperature (SST) trends in the Humboldt and California systems from 1982 to 2006. Lima and Wethey (2012) associated cooling SST trends in California and Humboldt upwelling systems with intensified upwelling from 1982 to 2010. Varela et al. (2018) found cooling SST trends in Benguela (− 0.25 °C dec^{-1}), Canary (− 0.3 °C dec^{-1}), Humboldt (− 0.3 °C dec^{-1}), and California (− 0.2 °C dec^{-1}) for 1982–2015. However, by mid-century, the EBUS landscape will shift as all EBUS will lose their ability to display cooling trends. Only the southern part of the Humboldt upwelling system (Chilean coast) and the Canary upwelling system are expected to exhibit lower-than-average SST warming rates, retaining their capacity to buffer global warming to some extent (ΔSST <0.8 °C). Conversely, the Peru, California, and Benguela upwelling systems are unlikely to show any upwelling influence on SST trends, with an expected SST rate of change up to 1.5 °C by mid-century. As a result, EBUS are projected to become more vulnerable to climate change, particularly in the southern hemisphere, due to the increased stress of marine heat waves (Wang et al., 2023).

4.2.2. Implications on marine ecosystems

Based on the main findings of this study, there are significant implications of the observed SST warming on various environmental factors. Changes in SST are linked with changes in acidification, dissolved oxygen, nutrients input, and the stratification of waters, among others (Allen et al., 2018). These impacts are expected to have the most significant effects on ecosystems in coastal locations, particularly in areas with the highest rates of SST warming observed in this study. The impact of SST warming is already being observed in various regions. For example, in the Norwegian Sea, salmonid farming has experienced significant shifts in productivity to colder northern waters, and commercial fish stocks have decreased in productivity due to the migration of species (Stenevik and Sundby, 2007; Hermansen and Heen, 2012). Similarly, the projected warming in the Scotian Shelf is exposing marine species in the area to significant vulnerability, with a decline of around 19–29 % in total biomass and 20–22 % in catches expected in the next 50 years (Guenette et al., 2014; Stortini et al., 2015). The fishing industry is already experiencing changes due to the SST increase, and studies have shown changes in fish catch patterns that will continue in the next decades (Cheung et al. (2013)).

The EBUS are of particular importance due to their significance in the biological realm as a thermal refuge against global warming (Seabra et al., 2019). As coastal warming increases, thermal stratification causes a decrease in the effectiveness of upwelling in pumping nutrient-rich waters, as reported by Bakun et al., 2015 and García-Reyes et al., 2015. Recent studies have already highlighted the potential impacts of global warming on EBUS. For instance, Rixen et al. (2021) found a decrease in oxygen levels and efficient nutrient trapping in the Benguela upwelling system. Sambe et al. (2016) investigated the productivity variations in the Canary Current Large Marine Ecosystem from 1997 to 2012 and reported declining trends in primary productivity, along with significant fishing pressure. In the Humboldt Upwelling System, climate change is expected to reduce small pelagic fish recruitment and cause changes in biomass and spatial distribution of fishery resources (Brochier et al., 2013; Gutiérrez et al., 2016), whereas similar results were observed for the California upwelling system (Arellano and Rivas, 2019). Nevertheless, these studies are limited by the models' ability to accurately represent the biogeochemical characteristics of the EBUS (Echevin et al., 2020).

4.3. Limitations

The current study utilized 17 CMIP6 GCMs with fine spatial resolution, which is crucial for capturing the characteristics of coastal areas. However, it is worth noting that significant SST biases exist in these models (Fox-Kemper et al., 2021), and they tend to overestimate nearshore SST in upwelling systems, making it difficult for them to reproduce coastal SST patterns (Varela et al., 2022a, 2022b). Therefore, we conducted our own SST bias correction process and included the results in Fig. S1 of the Supplementary Material.

Moreover, two different experiments have been considered in the present study: historical and hist-1950 experiments. The hist-1950 experiment has a higher resolution version of the CMIP6 models than the historical experiment. However, it is important to note that the improvement in the model's resolution is zone dependent, and higher resolution does not always guarantee more accurate results (Sylla et al., 2022; Varela et al., 2022b). In this study, models in the hist-1950 experiment showed slightly higher SST warming than those in the historical experiment, but the differences between the experiments were heterogeneous and varied across different basins. Nevertheless, the main findings of the study remain unchanged regardless of the experiment used.

5. Conclusions

Our results show a global, faster, and heterogeneous SST increase for worldwide coasts. SST increments around 1 °C for mid-century relative to 1995–2014 will be usual, with regions exceeding 2 °C. Regarding the Eastern Upwelling Boundary Systems, only the Canary upwelling system and the southern part of the Humboldt upwelling system manage to show lower-than-average SST warming rates, maintaining, to a certain extent, their ability to buffer global warming. Thus, the effects of SST warming that we are already seeing in the present will increase dramatically in the near future. The observed SST warming is expected to have significant impacts on the environment and ecosystems in coastal areas, with effects already being observed in the fishing industry. These findings highlight the urgent need for proactive measures to mitigate the impacts of climate change on our oceans and marine resources.

CRediT authorship contribution statement

R. Varela: Conceptualization, Methodology, Formal analysis, Investigation, Writing – original draft. **M. de Castro:** Conceptualization, Methodology, Investigation, Writing – review & editing, Supervision. **J.M. Dias:** Writing – review & editing, Supervision. **M. Gómez-Gesteira:** Conceptualization, Methodology, Writing – review & editing, Supervision.

Data availability

Data will be made available on request.

Declaration of competing interest

The authors declare that they have no known competing financial interests or personal relationships that could have appeared to influence the work reported in this paper.

Appendix A. Supplementary data

Supplementary data to this article can be found online at https://doi.org/10.1016/j.scitotenv.2023.164029.

References

Ahmed, N., Thompson, S., Glaser, M., 2019. Global aquaculture productivity, environmental sustainability, and climate change adaptability. Environ. Manag. 63, 159–172.
Alexander, M.A., Scott, J.D., Friedland, K.D., Mills, K.E., Nye, J.A., Pershing, A.J., Thomas, A.C., 2018. Projected sea surface temperatures over the 21st century: changes in the mean, variability and extremes for large marine ecosystem regions of northern oceans. Elementa: Sci. Anthropocene 6.
Allen, M.R., et al., 2018. Framing and Context. In: Masson-Delmotte, V., Zhai, P., Pörtner, H.-O., Roberts, D., Skea, J., Shukla, P.R., Pirani, A., Moufouma-Okia, W., Péan, C., Pidcock, R., Connors, S., Matthews, J.B.R., Chen, Y., Zhou, X., Gomis, M.I., Lonnoy, E., Maycock, T., Tignor, M., Waterfield, T. (Eds.), Global Warming of 1.5°C. An IPCC Special Report on the impacts of global warming of 1.5°C above pre-industrial levels and related global greenhouse gas emission pathways, in the context of strengthening the global response to the threat of climate change, sustainable development, and efforts to eradicate poverty. Cambridge University Press, Cambridge, UK and New York, NY, USA, pp. 49–92.
Alory, G., Wijffels, S., Meyers, G., 2007. Observed temperature trends in the Indian Ocean over 1960–1999 and associated mechanisms. Geophys. Res. Lett. 34, L02606.
Amengual, A., Homar, V., Romero, R., Alonso, S., Ramis, C., 2012. A statistical adjustment of regional climate model outputs to local scales: application to Platja de Palma, Spain. J. Climate 25 (3), 939–957.
Arellano, B., Rivas, D., 2019. Coastal upwelling will intensify along the Baja California coast under climate change by mid-21st century: insights from a GCM-nested physical-NPZD coupled numerical ocean model. J. Mar. Syst. 199, 103207.
Bakun, A., Black, B.A., Bograd, S.J., Garcia-Reyes, M., Miller, A.J., Rykaczewski, R.R., Sydeman, W.J., 2015. Anticipated effects of climate change on coastal upwelling ecosystems. Curr. Climate Change Rep. 1, 85–93.
Balaguru, K., Van Roekel, L.P., Leung, L.R., Veneziani, M., 2021. Subtropical eastern North Pacific SST bias in earth system models. J. Geophys. Res. Oceans 126 (8) e2021JC017359.
Belkin, I.M., 2009. Rapid warming of large marine ecosystems. Prog. Oceanogr. 81 (1–4), 207–213.
Benazzouz, A., et al., 2014. An improved coastal upwelling index from sea surface temperature using satellite-based approach–the case of the canary current upwelling system. Cont. Shelf Res. 81, 38–54.
Bock, L., et al., 2020. Quantifying progress across different CMIP phases with the ESMValTool. J. Geophys. Res.-Atmos. 125 (21).
Brickman, D., Hebert, D., Wang, Z., 2018. Mechanism for the recent ocean warming events on the Scotian shelf of eastern Canada. Cont. Shelf Res. 156, 11–22.
Brochier, T., Echevin, V., Tam, J., Chaigneau, A., Goubanova, K., Bertrand, A., 2013. Climate change scenarios experiments predict a future reduction in small pelagic fish recruitment in the Humboldt current system. Glob. Chang. Biol. 19 (6), 1841–1853.
Brown, J.N., Langlais, C., Gupta, A.S., 2015. Projected sea surface temperature changes in the equatorial Pacific relative to the warm Pool edge. Deep-Sea Res. II Top. Stud. Oceanogr. 113, 47–58.
Cai, W., et al., 2013. Projected response of the Indian Ocean dipole to greenhouse warming. Nat. Geosci. 6 (12), 999–1007.
Carvalho, K.S., Wang, S., 2020. Sea surface temperature variability in the Arctic Ocean and its marginal seas in a changing climate: patterns and mechanisms. Glob. Planet. Chang. 193, 103265.
Chamorro, A., Echevin, V., Dutheil, C., Tam, J., Gutiérrez, D., Colas, F., 2021. Projection of upwelling-favorable winds in the Peruvian upwelling system under the RCP8. 5 scenario using a high-resolution regional model. Clim. Dyn. 57, 1–16.
Cheng, L., Abraham, J., Hausfather, Z., Trenberth, K.E., 2019. How fast are the oceans warming? Science 363 (6423), 128–129.
Cheng, L., et al., 2022. Past and future ocean warming. Nature Rev. Earth Environ. 1-19.
Cheung, W.W.L., 2018. The future of fishes and fisheries in the changing oceans. J. Fish Biol. 92 (3), 790–803.
Cheung, W.W., Watson, R., Pauly, D., 2013. Signature of ocean warming in global fisheries catch. Nature 497 (7449), 365–368.
Cooley, S., et al., 2022. Oceans and Coastal Ecosystems and Their Services. In: Pörtner, H.-O., Roberts, D.C., Tignor, M., Poloczanska, E.S., Mintenbeck, K., Alegría, A., Craig, M., Langsdorf, S., Löschke, S., Möller, V., Okem, A., Rama, B. (Eds.), Climate Change 2022:

Impacts, Adaptation and Vulnerability. Contribution of Working Group II to the Sixth Assessment Report of the Intergovernmental Panel on Climate Change. Cambridge University Press, Cambridge, UK and New York, NY, USA, pp. 379–550.

Costanza, R., et al., 1997. The value of the world's ecosystem services and natural capital. Nature 387, 253–260.

Costoya, X., Rocha, A., Carvalho, D., 2020. Using bias-correction to improve future projections of offshore wind energy resource: a case study on the Iberian Peninsula. Appl. Energy 262, 114562.

Demarcq, H., 2009. Trends in primary production, sea surface temperature and wind in upwelling systems (1998–2007). Prog. Oceanogr. 83 (1–4), 376–385.

Des, M., Gómez-Gesteira, J.L., Decastro, M., Iglesias, D., Sousa, M.C., ElSerafy, G., Gómez-Gesteira, M., 2022. Historical and future naturalization of Magallana gigas in the Galician coast in a context of climate change. Sci. Total Environ. 838, 156437.

Dunstan, P.K., et al., 2018. Global patterns of change and variation in sea surface temperature and chlorophyll a. Sci. Rep. 8 (1), 1–9.

Echevin, V., Gévaudan, M., Espinoza-Morriberón, D., Tam, J., Aumont, O., Gutierrez, D., Colas, F., 2020. Physical and biogeochemical impacts of RCP8. 5 scenario in the Peru upwelling system. Biogeosciences 17 (12), 3317–3341.

Eyring, V., Bony, S., Meehl, G.A., Senior, C.A., Stevens, B., Stouffer, R.J., Taylor, K.E., 2016. Overview of the coupled model Intercomparison project phase 6 (CMIP6) experimental design and organization. Geosci. Model Dev. 9, 1937–1958.

Farneti, R., Stiz, A., Ssebandeke, J.B., 2022. Improvements and persistent biases in the southeast tropical Atlantic in CMIP models. npj Climate and Atmospheric Science 5 (1), 1–11.

Fox-Kemper, B., et al., 2021. Ocean, Cryosphere and Sea Level Change. In: Masson-Delmotte, V., Zhai, P., Pirani, A., Connors, S.L., Péan, C., Berger, S., Caud, N., Chen, Y., Goldfarb, L., Gomis, M.I., Huang, M., Leitzell, K., Lonnoy, E., Matthews, J.B.R., Maycock, T.K., Waterfield, T., Yelekçi, O., Yu, R., Zhou, B. (Eds.), Climate Change 2021: The Physical Science Basis. Contribution of Working Group I to the Sixth Assessment Report of the Intergovernmental Panel on Climate Change. Cambridge University Press, Cambridge, United Kingdom and New York, NY, USA, pp. 1211–1362.

Galappaththi, E.K., Ichien, S.T., Hyman, A.A., Aubrac, C.J., Ford, J.D., 2020. Climate change adaptation in aquaculture. Rev. Aquac. 12 (4), 2160–2176.

García-Reyes, M., Sydeman, W.J., Schoeman, D.S., Rykaczewski, R.R., Black, B.A., Smit, A.J., Bograd, S.J., 2015. Under pressure: climate change, upwelling, and eastern boundary upwelling ecosystems. Front. Mar. Sci. 2, 109.

Gray, J.S., 1997. Marine biodiversity: patterns, threats and conservation needs. Biodivers. Conserv. 6 (1), 153–175.

Guenette, S., Araujo, J.N., Bundy, A., 2014. Exploring the potential effects of climate change on the Western Scotian shelf ecosystem, Canada. J. Marine Syst. 134, 89–100.

Gutiérrez, D., Bouloubassi, I., Sifeddine, A., Purca, S., Goubanova, K., Graco, M., ... Ortlieb, L., 2011. Coastal cooling and increased productivity in the main upwelling zone off Peru since the mid-twentieth century. Geophys. Res. Lett. 38 (7).

Gutiérrez, D., Akester, M., Naranjo, L., 2016. Productivity and sustainable management of the Humboldt current large marine ecosystem under climate change. Environ. Dev. 17, 126–144.

Haarsma, R.J., et al., 2016. High resolution model intercomparison project (HighResMIP v1. 0) for CMIP6. Geosci. Model Dev. 9 (11), 4185–4208.

Halpern, B.S., et al., 2008. A global map of human impact on marine ecosystems. Science 319, 948–952.

Hansen, J., Ruedy, R., Sato, M., Lo, K., 2010. Global surface temperature change. Rev. Geophys. 48 (4).

Harvey, N., 2006. In: Glazer, M.P. (Ed.), Rates and Impacts of global sea Level Change. New Frontiers in Environmental Research. Nova Science Publishers, Hauppage, New York.

Hermansen, Ø., Heen, K., 2012. Norwegian salmonid farming and global warming: socioeconomic impacts. Aquac. Econ. Manag. 16 (3), 202–221.

Hobday, A.J., Lough, J.M., 2011. Projected climate change in Australian marine and freshwater environments. Mar. Freshw. Res. 62 (9), 1000–1014.

Hobday, A.J., Pecl, G.T., 2014. Identifcation of global marine hotspots: sentinels for change and vanguards for adaptation action. Rev. Fish Biol. Fish. 24, 215–225.

Hoegh-Guldberg, O., et al., 2018. Impacts of 1.5°C Global Warming on Natural and Human Systems. In: Masson-Delmotte, V., Zhai, P., Pörtner, H.-O., Roberts, D., Skea, J., Shukla, P.R., Pirani, A., Moufouma-Okia, W., Péan, C., Pidcock, R., Connors, S., Matthews, J.B.R., Chen, Y., Zhou, X., Gomis, M.I., Lonnoy, E., Maycock, T., Tignor, M., Waterfield, T. (Eds.), Global Warming of 1.5°C. An IPCC Special Report on the impacts of global warming of 1.5°C above pre-industrial levels and related global greenhouse gas emission pathways, in the context of strengthening the global response to the threat of climate change, sustainable development, and efforts to eradicate poverty. Cambridge University Press, Cambridge, UK and New York, NY, USA, pp. 175–312.

Hoegh-Guldberg, O. & Bruno, J. F. The impact of climate change on the world's marine ecosystems. Science, 328 (5985) (2010), pp. 1523–1528 (2010).

Hoegh-Guldberg, O., et al., 2014. The Ocean. In: Barros, V.R., Field, C.B., Dokken, D.J., Mastrandrea, M.D., Mach, K.J., Bilir, T.E., Chatterjee, M., Ebi, K.L., Estrada, Y.O., Genova, R.C., Girma, B., Kissel, E.S., Levy, A.N., MacCracken, S., Mastrandrea, P.R., White, L.L. (Eds.), Climate Change 2014: Impacts, Adaptation, and Vulnerability. Part B: Regional Aspects. Contribution of Working Group II to the Fifth Assessment Report of the Intergovernmental Panel on Climate Change. Cambridge University Press, Cambridge, United Kingdom and New York, NY, USA, pp. 1655–1731.

Huang, B., L'Heureux, M., Hu, Z.Z., Zhang, H.M., 2016. Ranking the strongest ENSO events while incorporating SST uncertainty. Geophys. Res. Lett. 43 (17), 9165–9172.

IPCC, 2014. In: Barros, V.R., Field, C.B., Dokken, D.J., Mastrandrea, M.D., Mach, K.J., Bilir, T.E., et al. (Eds.), Climate Change 2014: Impacts, Adaptation, and Vulnerability. Part B: Regional Aspects. Contribution of Working Group II to the Fifth Assessment Report of the Intergovernmental Panel of Climate. Cambridge University Press, Cambridge.

IPCC, 2018. Summary for Policymakers. In: Masson-Delmotte, V., Zhai, P., Pörtner, H.-O., Roberts, D., Skea, J., Shukla, P.R., Pirani, A., Moufouma-Okia, W., Péan, C., Pidcock, R., Connors, S., Matthews, J.B.R., Chen, Y., Zhou, X., Gomis, M.I., Lonnoy, E., Maycock, T., Tignor, M., Waterfield, T. (Eds.), Global Warming of 1.5°C. An IPCC Special Report on the impacts of global warming of 1.5°C above pre-industrial levels and related global greenhouse gas emission pathways, in the context of strengthening the global response to the threat of climate change, sustainable development, and efforts to eradicate poverty. Cambridge University Press, Cambridge, UK and New York, NY, USA, pp. 3–24.

IPCC, 2021. In: Masson-Delmotte, V., Zhai, P., Pirani, A., Connors, S.L., Péan, C., Berger, S., Caud, N., Chen, Y., Goldfarb, L., Gomis, M.I., Huang, M., Leitzell, K., Lonnoy, E., Matthews, J.B.R., Maycock, T.K., Waterfield, T., Yelekçi, O., Yu, R., Zhou, B. (Eds.), Climate Change 2021: The Physical Science Basis. Contribution of Working Group I to the Sixth Assessment Report of the Intergovernmental Panel on Climate Change. Cambridge University Press, Cambridge, United Kingdom and New York, NY, USA, p. 2391.

Kessler, A., Goris, N., Lauvset, S.K., 2022. Observation-Based Sea surface temperature trends in Atlantic large marine ecosystems. Prog. Oceanogr. 208, 102902.

Khan, A.H., Levac, E., Chmura, G.L., 2013. Future Sea surface temperatures in large marine ecosystems of the Northwest Atlantic. ICES J. Mar. Sci. 70 (5), 915–921.

Lee, J.-Y., et al., 2021. Future Global Climate: Scenario-Based Projections and Near Term Information. In: Masson-Delmotte, V., Zhai, P., Pirani, A., Connors, S.L., Péan, C., Berger, S., Caud, N., Chen, Y., Goldfarb, L., Gomis, M.I., Huang, M., Leitzell, K., Lonnoy, E., Matthews, J.B.R., Maycock, T.K., Waterfield, T., Yelekçi, O., Yu, R., Zhou, B. (Eds.), Climate Change 2021: The Physical Science Basis. Contribution of Working Group I to the Sixth Assessment Report of the Intergovernmental Panel on Climate Change. Cambridge University Press, Cambridge, United Kingdom and New York, NY, USA, pp. 553–672.

Li, J.L., et al., 2020. An overview of CMIP5 and CMIP6 simulated cloud ice, radiation fields, surface wind stress, sea surface temperatures, and precipitation over tropical and subtropical oceans. J. Geophys. Res.-Atmos. 125 (15) e2020JD032848.

Lima, F.P., Wethey, D.S., 2012. Three decades of high-resolution coastal sea surface temperatures reveal more than warming. Nat. Commun. 3 (1), 1–13.

Ma, J., Xu, S., Wang, B., 2019. Warm bias of sea surface temperature in eastern boundary current regions—a study of effects of horizontal resolution in CESM. Ocean Dyn. 69 (8), 939–954.

Oliver, E.C., Wotherspoon, S.J., Chamberlain, M.A., Holbrook, N.J., 2014. Projected Tasman Sea extremes in sea surface temperature through the twenty-first century. J. Clim. 27 (5), 1980–1998.

Oliver, E.C., et al., 2019. Projected marine heatwaves in the 21st century and the potential for ecological impact. Front. Mar. Sci. 6, 734.

Oliver, E.C., et al., 2021. Marine heatwaves. Annu. Rev. Mar. Sci. 13, 313–342.

Overland, J.E., Wang, M., 2007. Future climate of the North Pacific Ocean. EOS Trans. Am. Geophys. Union 88 (16), 178–182.

Park, W., Latif, M., 2020. Resolution dependence of CO2-induced tropical Atlantic sector climate changes. Npj Climate and Atmospheric Science 3 (1).

Pauly, D., Christensen, V., 1995. Primary production required to sustain global fisheries. Nature 374 (6519), 255–257.

Rao, S.A., Dhakate, A.R., Saha, S.K., Mahapatra, S., Chaudhari, H.S., Pokhrel, S., Sahu, S.K., 2012. Why is Indian Ocean warming consistently? Clim. Chang. 110 (3), 709–719.

Richter, I., Tokinaga, H., 2020. An overview of the performance of CMIP6 models in the tropical Atlantic: mean state, variability, and remote impacts. Clim. Dyn. 55 (9), 2579–2601.

Rixen, T., et al., 2021. Oxygen and nutrient trapping in the southern Benguela upwelling system. Front. Mar. Sci. 8, 730591.

Roxy, M.K., Ritika, K., Terray, P., Masson, S., 2014. The curious case of Indian Ocean warming. J. Clim. 27 (22), 8501–8509.

Roxy, M.K., et al., 2020. Indian ocean warming. Assessment of Climate Change over the Indian Region. Springer, Singapore, pp. 191–206.

Ruela, R., Sousa, M.C., de Castro, M., Dias, J.M., 2020. Global and regional evolution of sea surface temperature under climate change. Glob. Planet. Chang. 190, 103190.

Sambe, B., Tandstad, M., Caramelo, A.M., Brown, B.E., 2016. Variations in productivity of the canary current large marine ecosystem and their effects on small pelagic fish stocks. Environ. Dev. 17, 105–117.

Santos, F., Gómez-Gesteira, M., de Castro, M., Álvarez, I., 2012. Differences in coastal and oceanic SST warming rates along the canary upwelling ecosystem from 1982 to 2010. Cont. Shelf Res. 47, 1–6.

Sasaki, Y.N., Umeda, C., 2021. Rapid warming of sea surface temperature along the Kuroshio and the China coast in the East China Sea during the twentieth century. J. Clim. 34 (12), 4803–4815.

Scannell, H.A., Pershing, A.J., Alexander, M.A., Thomas, A.C., Mills, K.E., 2016. Frequency of marine heatwaves in the North Atlantic and North Pacific since 1950. Geophys. Res. Lett. 43 (5), 2069–2076.

Seabra, R., Varela, R., Santos, A.M., Gomez-Gesteira, M., Meneghesso, C., Wethey, D.S., Lima, F.P., 2019. Reduced nearshore warming associated with eastern boundary upwelling systems. Front. Mar. Sci. 6, 104.

Seidov, D., Mishonov, A., Parsons, R., 2021. Recent warming and decadal variability of gulf of Maine and slope water. Limnol. Oceanogr. 66 (9), 3472–3488.

Smith, K.E., et al., 2022. Biological impacts of marine heatwaves. Annu. Rev. Mar. Sci. 15.

Stenevik, E.K., Sundby, S., 2007. Impacts of climate change on commercial fish stocks in Norwegian waters. Mar. Policy 31 (1), 19–31.

Stortini, C.H., Shackell, N.L., Tyedmers, P., Beazley, K., 2015. Assessing marine species vulnerability to projected warming on the Scotian shelf, Canada. ICES J. Marine Sci. 72 (6), 1731–1743.

Sylla, A., Gomez, E.S., Mignot, J., López-Parages, J., 2022. Impact of increased resolution on the representation of the canary upwelling system in climate models. Geosci. Model Dev. 15, 8245–8267.

Taylor, K.E., Stouffer, R.J., Meehl, G.A., 2012. An overview of CMIP5 and the experiment design. Bull. Am. Meteorol. Soc. 93 (4), 485–498.

Varela, R., Lima, F.P., Seabra, R., Meneghesso, C., Gómez-Gesteira, M., 2018. Coastal warming and wind-driven upwelling: a global analysis. Sci. Total Environ. 639, 1501–1511.

Varela, R., Rodríguez-Díaz, L., de Castro, M., Gómez-Gesteira, M., 2022a. Influence of canary upwelling system on coastal SST warming along the 21st century using CMIP6 GCMs. Glob. Planet. Chang. 208, 103692.

Varela, R., de Castro, M., Rodriguez-Diaz, L., Dias, J.M., Gómez-Gesteira, M., 2022b. Examining the ability of CMIP6 models to reproduce the upwelling SST imprint in the eastern boundary upwelling systems. J. Marine Sci. Eng. 10 (12), 1970.

Wang, C., Zhang, L., Lee, S.K., Wu, L., Mechoso, C.R., 2014. A global perspective on CMIP5 climate model biases. Nat. Clim. Chang. 3, 201–205.

Wang, Y., Heywood, K.J., Stevens, D.P., Damerell, G.M., 2022. Seasonal Extrema of sea surface temperature in CMIP6 models. Ocean Sci. 18 (3), 839–855.

Wang, S., et al., 2023. Southern hemisphere eastern boundary upwelling systems emerging as future marine heatwave hotspots under greenhouse warming. Nat. Commun. 14 (1), 28.

Watson, R.A., Cheung, W.W., Anticamara, J.A., Sumaila, R.U., Zeller, D., Pauly, D., 2013. Global marine yield halved as fishing intensity redoubles. Fish Fish. 14 (4), 493–503.

Wei, Y., et al., 2023. The weakened upwelling at the upstream Kuroshio in the East China Sea induced extensive sea surface warming. Geophys. Res. Lett. 50 (1) e2022GL101835.

Worm, B., et al., 2009. Rebuilding global fisheries. Science 325 (5940), 578–585.